A Silver-Modified Copper Foam Electrode for Electrochemical Dehalogenation Using Mono-Bromoacetic Acid as an Indicator

Zhiqiao He, Qiong Wang, Junjun Sun, Jianmeng Chen, Shuang Song[*]

College of Biological and Environmental Engineering, Zhejiang University of Technology, Hangzhou 310032, People's Republic of China
[*]E-mail: ss@zjut.edu.cn

To improve the effectiveness of dehalogenation of organic halogen compounds, a series of silver-modified Cu foam electrodes (Ag/Cu foam electrode) was prepared via chemical deposition, using $AgNO_3$ as the precursor. The crystal structure and morphology of the electrodes were measured by means of X-ray diffraction (XRD) and scanning electron microscopy (SEM). It was found that zero-valence Ag particles dispersed finely on the Cu foam surface and their number increased with Ag loading. Electrocatalytic activity was evaluated by monitoring the debromination of mono-bromoacetic acid (MBAA). The best operational conditions were a silver loading of 2 mg/cm^2, applied current density of 5.5 mA/cm^2, and pH 7.0. After five successive cycles, the Ag/Cu electrode remained stable for the electrocatalytic debromination of MBAA. We suggest that the improved electrocatalytic activity of the Ag/Cu electrode is mainly attributable to a strong interaction between MBAA and the Ag particles on the surface of electrode. These findings might be of great significance for improving the electrochemical dehalogenation process.
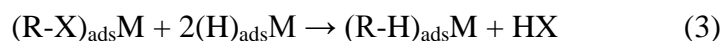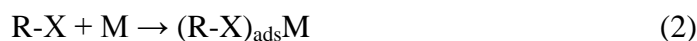
1. INTRODUCTION

Electrocatalytic reductive dehalogenation is widely considered to be a promising technique for the detoxification and disposal of industrial effluents containing organic halides [1-10]. This method has many attractive advantages over other reductive pathways, including, zero-valent iron [11, 12], microbial reduction [13], and photocatalytic dehalogenation [14, 15], because it is relatively milder, more selective, and easier to operate, particularly with respect to catalyst recovery [4].

According to the literature [16-18], electrocatalytic hydrogenolysis (ECH) involves a process described in Eqs. (1)–(4), where M denotes the metallic surface and $(H)_{ads}M$ represents the chemisorbed hydrogen.

$$2H_2O + 2e^- + M \rightarrow 2(H)_{ads}M + 2OH^- \tag{1}$$

$$R\text{-}X + M \rightarrow (R\text{-}X)_{ads}M \tag{2}$$

$$(R\text{-}X)_{ads}M + 2(H)_{ads}M \rightarrow (R\text{-}H)_{ads}M + HX \tag{3}$$

$$(R\text{-}H)_{ads}M \rightarrow R\text{-}H + M \tag{4}$$

As shown above, there are four reaction steps in the dehalogenation, *i.e.*, (1) The formation of chemisorbed hydrogen, $(H)_{ads}M$, on the metal cathode surface, by the reduction of water via the Volmer reaction, (2) the adsorption of organic halogenation onto the metal surface, (3) hydrogenolysis of the R–X bond by catalytic hydrogenation, through a reaction between $(H)_{ads}M$ and the adsorbed substrate $(R–X)_{ads}M$, and (4) the regeneration of the metal surface via desorption of the products generated in Eq. (3).

ECH always competes with the hydrogen evolution reaction (HER), which proceeds either via the Volmer-Heyrovsky reaction, Eq. (5), or the Volmer-Tafel mechanism, Eq. (6).

$$(H)_{ads}M + H_2O + e^- \rightarrow H_2 + M + OH^- \tag{5}$$

$$(H)_{ads}M + (H)_{ads}M \rightarrow H_2 + 2M \tag{6}$$
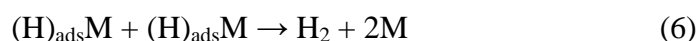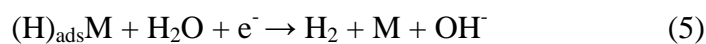
Various metals have been employed as appropriate catalysts for the electrochemical reductive dehalogenation of organic halogenation, including, lead [2], zinc [3], copper [19-23], and palladium [5-7, 23-25]. However, more efficient catalysts are still urgently required. Recent research has addressed the reduction of polyhalogenated phenols using Ag electrodes [1, 4, 10].

The surface morphology of the electrode plays an important role in the electrocatalytic process and large surface areas are generally preferred for many supported catalysts [26], so more attention might be paid to the application of Ag particles for the provision of a very large number of active sites. The selection of appropriate support materials to separate the catalytic particles and prevent their agglomeration appears to be of great importance when meeting this objective [27]. Support materials normally used as cathode substrates include various carbon materials [28-32], different metal materials [24, 33, 34], and polypyrrole [18]. Metal foams exhibit a three dimensional (3-D) network structure with micro-open cages, which further enlarge the surface area and allow the catalyst particles to be deposited firmly on the surface. The 3-D architecture also offers great potential for rapid electrochemical reactions, because of the extremely large specific surface area available for charge and mass transfer [34].

The primary objective of this study was to prepare and characterize an Ag-modified foam electrode (Ag/Cu foam electrode). This study also elucidated the effects of different operating parameters, including, Ag loading, current density, and pH, on the dehalogenation of mono-bromoacetic acid (MBAA). The activity and stability of the electrode was explored, so as to assess the possibility of successive reductive dehalogenation. Cu foam was chosen as the substrate, because it is a good candidate for use as a negative electrode material in ECH [35].

2. EXPERIMENTAL

2.1. Materials and reagents

The Cu foam (Shenzhen Rolinsia Power Materials Co. Ltd, China) was cleaned by sonication in acetone and dilute hydrochloric acid, before being used as the substrate for silver deposition. $AgNO_3$ (Shanghai Chemical Reagent Co. Ltd., China) was used for the chemical deposition of silver particles onto the Cu foam substrate. The model substance, MBAA, was obtained from Aladdin Chemical Reagent Co. Ltd., China. Nitrogen (purity 99.99%) was supplied by Hangzhou Jingong Special Gas Co. Ltd., China. All the other chemicals, including, NaH_2PO_4, Na_2HPO_4, acetone, and NaCl, were analytically pure and purchased from Huadong Medical Co. Ltd., China. All solutions used during synthesis and treatment were prepared using deionized, doubly-distilled water.

2.2. Electrode preparation and characterization

During chemical deposition of silver, a Cu foam (20 mm × 30 mm; thickness, 1.0 mm) support was placed into a 100 ml conical flask containing 60 ml of $AgNO_3$ aqueous solution in the concentration range 1.67–150 mg/L. The conical flask was then capped and placed in an incubator shaker for 1 h at 30 °C. The resulting Ag/Cu foam was stored in methanol for later use, so as to avoid oxidation [24].

X-ray diffraction (XRD) patterns were collected using a Thermo ARL Scintag X'TRA X-ray diffractometer with Cu $K\alpha$ radiation (wavelength = 1.54178 nm), operating at 40 kV and 40 mA with a scan rate of 2.0°/min. Scanning electron microscopy (SEM) photographs were obtained using a field emission Philips XL-30 operated at 15 kV.

2.3. Bulk Electrolysis

Electrolysis was carried out in a two-compartment cell with effective electrolyte volumes of 60 and 35 ml, which were divided by a Nafion-117 cation exchange membrane to prevent bromide ions produced in the cathode compartment from diffusing into the anode compartment. Ag/Cu foam electrodes were used as cathodes to reduce 10 mM MBAA and a platinum foil (20 mm × 30 mm × 3 mm) was used as the counter-electrode. The distance between the anode and the cathode was about 80 mm.

A stock solution of MBAA was prepared before each run. Different initial pH values (4.0, 7.0, and 12.0) of simulated wastewater containing aqueous MBAA were obtained by adjusting the phosphate buffer. The electrocatalytic reduction was carried out by batch processing conducted at current densities of 1.5, 3.5, 5.5, 7.5, and 9.5 mA/cm^2. The cathodic compartment was kept in a non-oxidizing atmosphere by sparging with nitrogen before and during the debromination experiment. Samples (1 ml) of catholyte were periodically withdrawn from the cathode compartment to determine product analysis at predetermined time-points during electrolysis.

2.4. Analytical methods

The concentrations of MBAA, acetic acid, and bromide ions generated during electrolysis were identified by ion chromatography (IC). Measurements were made with an ion chromatography (IC) system (ICS-2000) equipped with a dual-piston (in series) pump, a Dionex IonPac AS19 analytical column (4 mm × 250 mm), and an IonPac AG19 guard column (4 mm × 250 mm). Detection was performed with a Dionex DS6 conductivity detector. Suppression of the eluent was achieved using an anion electrolytic suppressor (4 mm ASRS, Dionex, USA), which was operated in the external water mode.

3. RESULTS AND DISCUSSION

3.1. Characterization of electrodes

XRD spectra of Cu foam and Ag/Cu foam electrodes are shown in Fig. 1.
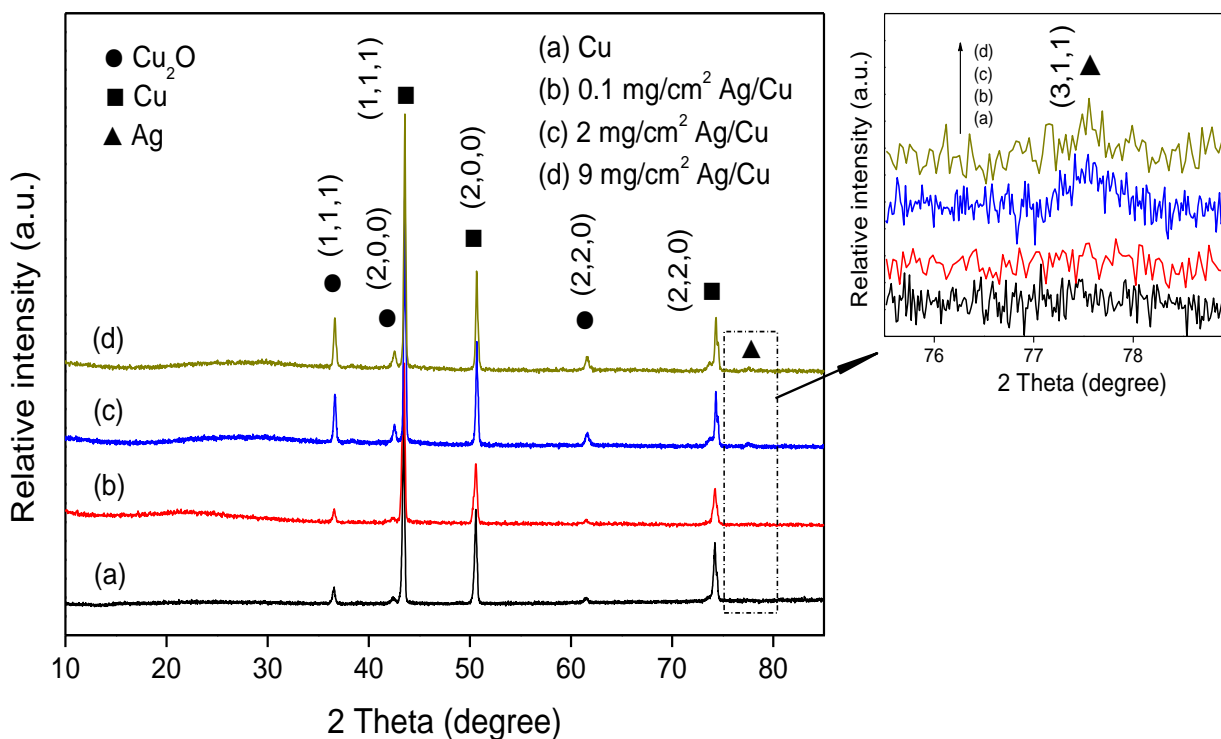
Figure 1. XRD patterns of Cu foam (a), 0.1 mg/cm^2 Ag/Cu foam (b), 2 mg/cm^2 Ag/Cu foam (c) and 9 mg/cm^2 Ag/Cu foam electrodes (d).

All of the samples clearly showed diffraction from the (1, 1, 1), (2, 0, 0) and (2, 2, 0) planes of copper metal (PDF no. 001-1242), with respect to the 2θ values of approximately 43.5°, 50.7°, and 74.7°, respectively. A diffraction peak at 77.4°, as shown in the inset of Fig. 1, was observed for the

Ag/Cu foam electrode, which was assigned to the (3, 1, 1) phase of Ag^0 (PDF no. 087-0717). This indicates that silver particles could be successfully deposited onto the Cu foam surface by chemical deposition. Note that the weak (1, 1, 1), (2, 0, 0) and (2, 2, 0) planes of Cu_2O (PDF no. 001-1142) appeared in all samples, which indicates the presence of Cu_2O on the surface of the Cu foam. The undesirable phases of Cu_2O might have originated from the preparation of copper foam.
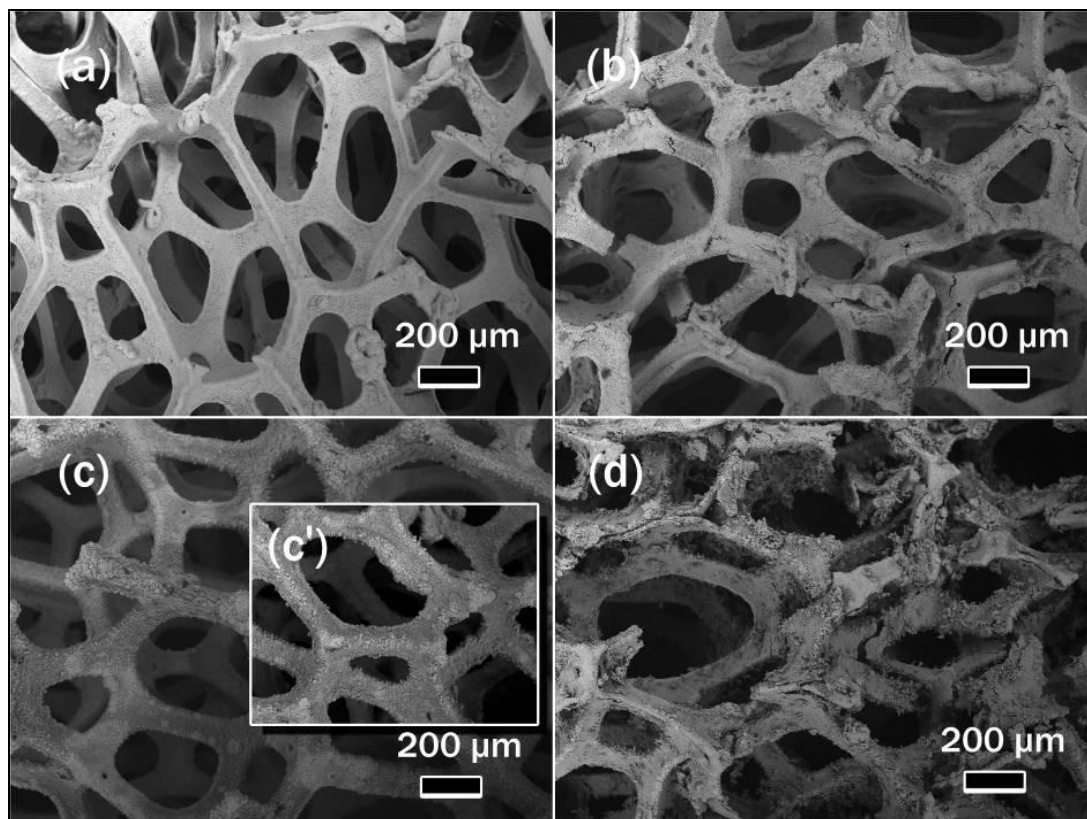

Figure 2. SEM images of fresh Cu foam (a), 0.1 mg/cm^2 Ag/Cu foam (b), 2 mg/cm^2 Ag/Cu foam (c) and 9 mg/cm^2 Ag/Cu foam (d) electrodes, and the 2 mg/cm^2 Ag/Cu foam (c') electrode after five debromination cycles.

SEM is a widely used surface analysis technique, which examines the surface morphology of solids rapidly, but without damaging the surface. Fig. 2 shows typical SEM surface morphology images of the Cu foam and the Ag/Cu foam electrodes. As shown in Fig. 2a, the Cu foam was smooth and formed a reticular structure with 3-D cross-linked pores with a mean pore size of about 300 μm. It was obvious from the mass contrast that there were dense particles that consisted of well dispersed silver particles on the surface of the Cu foam (Panels b-d), thereby enlarging the surface area of the catalysts [36].

SEM images of foam electrodes that were used five times are shown in Fig. 2c'. Fig. 2c' shows that silver particles persisted on the surface of the Cu foam, which suggests that silver particles did not desquamate from the Ag/Cu foam electrode after debromination.

3.2. Comparasion of the electrocatalytic activities of the Ag/Cu and Cu foam electrode

The electrocatalytic activity of the Cu foam was evaluated with and without silver modification, using 10 mM MBAA in neutral phosphate buffer.
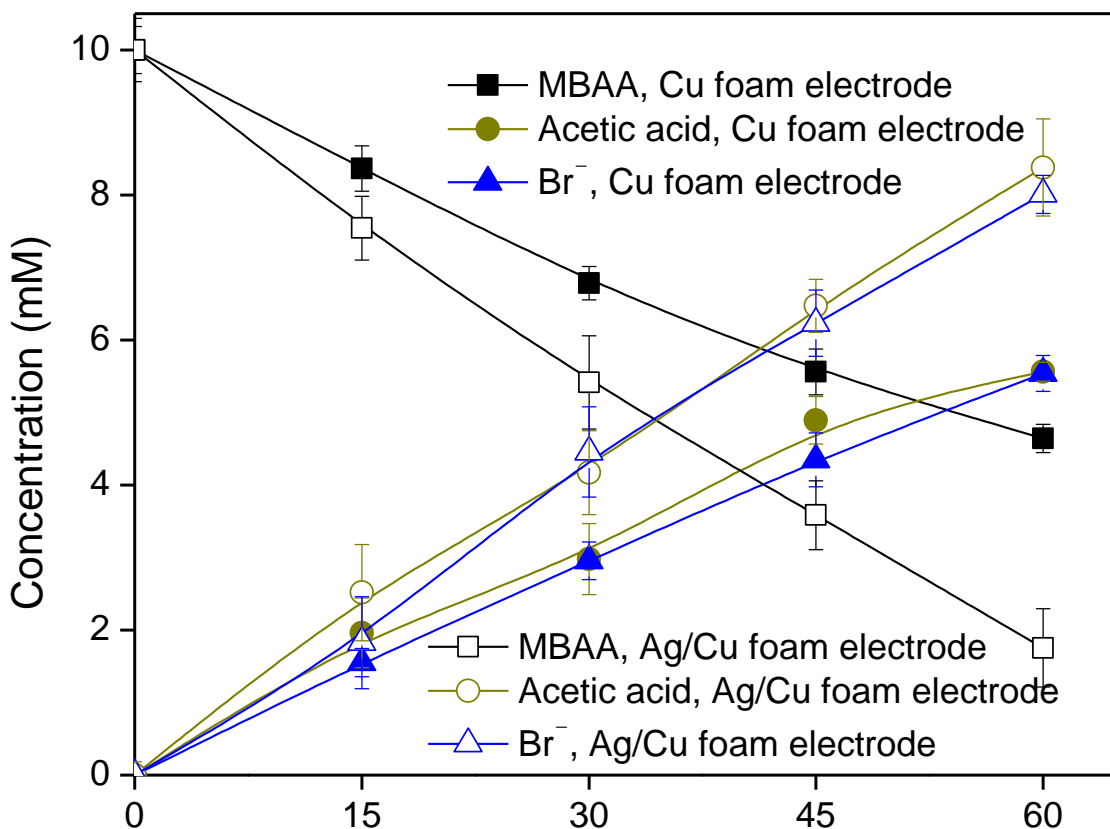
Figure 3. Variation of the concentration of MBAA, acetic acid, and Br$^-$ during the electrochemical debromination process with the Cu foam and the Ag/Cu foam electrodes: initial concentration of MBAA, 10 mM; silver loading, 2 mg/cm^2; current density, 5.5 mA/cm^2; pH 7.0.

Fig. 3 shows the efficiency of the electrocatalytic conversion for MBAA after 1 h. Cu foam showed favorable debromination ability in this reaction system. Earlier studies showed that Cu can serve as an available electron donor for the dehalogenation of organohalogen compounds [20-22, 37, 38]. Compared with the Cu foam electrode, the electrocatalytic activity was enhanced markedly after the loading with Ag. The following hypotheses are proposed to account for the increased debromination efficiency. Elemental silver is prone to adsorbing halogenated organics, which leads to the formation of bridge-like R . . . X . . . Ag intermediates between the substrate and the metal surface [4, 10]. Thus, the transfer of MBAA from the bulk solution to the surface Ag particles was improved, thereby accelerating the debromination rate.

3.3. Analysis of MBAA debromination mass balance

To provide a better understanding of the mechanism of MBAA debromination, a mass balance analysis was performed on the basis of quantitative determination of MBAA, acetic acid, and Br$^-$. The results are shown in Fig. 3. It was determined that acetic acid and Br$^-$ were formed and increased steadily. With a silver loading of 2 mg/cm^2, current density of 5.5 mA/cm^2, and pH of 7.0, the MBAA concentration decreased rapidly from 10 to 1.75 mM on the Ag/Cu electrode after 1 h reaction. The molar concentration of the MBAA removed was almost equal to that of the acetic acid produced, which also matched that of the Br$^-$ formed. The total amounts of Br$^-$ and carbon before and after the reaction remained almost unchanged, which indicates that acetic acid and Br$^-$ are primary debromination products.

3.4. Effect of operating variables

3.4.1. Effect of silver loading

The Ag loading, expressed as the weight of Ag based on the Cu electrode area, was varied from 0.1 mg/cm^2 to 9 mg/cm^2 to study the effect of Ag loading on electrocatalytic debromination.
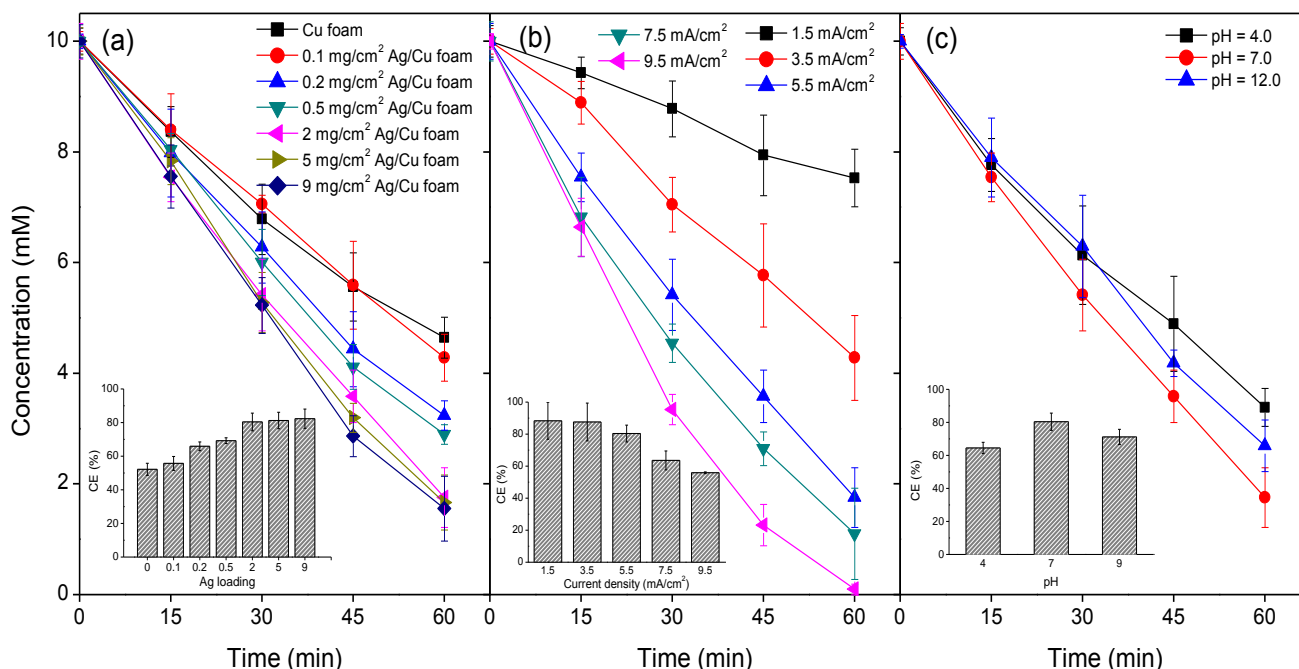
Figure 4. Effect of process variables on the debromination of MBAA. (a) Effect of silver loading: pH 7.0; current density, 5.5 mA/cm^2. (b) Effect of current density: pH 7.0; silver loading, 2 mg/cm^2. (c) Effect of pH: current density, 5.5 mA/cm^2; silver loading, 2 mg/cm^2.

Fig. 4a indicates the decrement of MBAA and current efficiency under a controlled current density of 5.5 mA/cm^2 after 1 h electrolysis. It is clear that an optimum catalyst loading state was found. When Ag loading was relatively low, the reactions on the surface of the Ag controlled the whole process and highly reactive hydrogen bound on the Ag surface were insufficient for debromination [35]. As the Ag loading was increased, the MBAA conversion significantly increased, with 2 mg/cm^2 Ag/Cu delivering the highest conversion rate and current efficiency. From the observed reaction rate, we concluded that any further increase in Ag loading would have only slight positive effects on the debromination of MBAA and current efficiency.

As demonstrated by the SEM results above, Ag particles dispersed on the surface of Cu foam increased with increased silver loading. When the Ag loading was higher than 2 mg/cm^2, Ag particles covered the surface of Cu electrode to excess, which caused the aggregation of Ag particles and the formation of larger sized Ag clusters. By combining these findings the results given above, we determined that the optimum for silver loading was 2 mg/cm^2.

3.4.2. Effect of current density

Fig. 4b shows the decrease of MBAA in the catholyte for different current densities during electrolysis. By increasing the current density from 1.5 to 9.5mA/cm^2 it was shown that the rate of MBAA conversion, in terms of the amount of MBAA removed, was higher at a higher current density after 1 h electrolysis. According to Eqs. (1)–(2), the increased current density enhances the formation of $(H)_{ads}M$, which in turn promotes the reductive debromination of MBAA. However, the current efficiency of the process was decreased with the increase of current density. This was principally due to the hydrogen evolution side-reaction, which was strongly dependent on current density. At high current densities, the rate of $(H)_{ads}M$ became faster than the rate at which MBAA could be transported to the surface of the Ag particles and be adsorbed. Consequently, a greater proportion of $(H)_{ads}M$ tended to participate in the unfavorable reaction of hydrogen gas evolution [6].

3.4.3. Effect of pH

The degradation experiment to test the effect of pH was repeated under acid (pH 4.0), neutral (pH 7.0), and basic (pH 12.0) conditions. It is clear from Fig. 4c that debromination was pH-dependent and that the debromination rate was highest when the pH was 7.0. Higher or lower pH inhibited electrocatalytic activity. The variation of the current efficiency found the same trend. The reaction kinetics of the Volmer step (Eq. (1)) supported the positive influence of acid solution. The production of active hydrogen appears to be most feasible, by promoting the formation of $(H)_{ads}M$ and affecting the subsequent rate of hydrogenation, as in Eqs. (3) and (4). Thus, the efficiency of the electrocatalytic reduction was enhanced. In contrast, the reaction kinetics of Volmer step and Tafel step, Eq. (1) and Eq. (6), were also accelerated. Hence, an excess of $(H)_{ads}M$ leads to the formation of H$_2$ layers, which occupy active metal sites on the surface of the electrode, thereby preventing the adsorption of MBAA

onto the electrode. Synthesizing these findings, the most beneficial condition for increasing the debromination of MBAA was a neutral condition [39].

3.5. Evaluation of electrode stability

Good electrode stability is an important factor determining the choice of an ideal electrode. Electrode stability was evaluated, based on the change of debromination rate after five consecutive cycles.
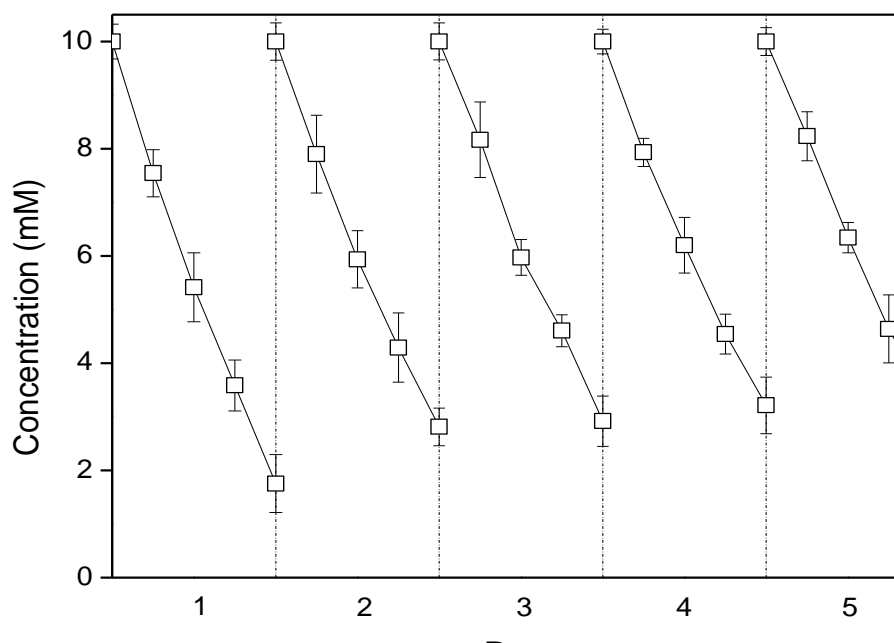
Figure 5. Variation of MBAA debromination by the Ag/Cu foam electrode after five debromination cycles: initial concentration of MBAA, 10 mM; silver loading, 2 mg/cm^2; current density, 5.5 mA/cm^2; pH 7.0.

Fig. 5 shows that the conversion of MBAA decreased from 71.9% to 67.6% after the electrode was used five times. Thus the Ag/Cu foam electrode retained a sufficiently high stability, because the debromination rate only marginally deteriorated on repeated use. The Ag/Cu electrode was also observed using the SEM after five uses, but no obvious damage or changes in the structure or morphology were observed.

4. CONCLUSIONS

In summary, the Ag/Cu electrode exhibited an effective electrocatalytic debromination capacity for the reduction of MBAA in aqueous solution. An integrated analysis of removal efficiency and

current efficiency found that a silver loading of 2 mg/cm^2, debromination current density of 5.5 mA, and a pH of 7.0 were the optimum debromination conditions. It was deduced that a strong interaction occurred between MBAA and the reactive sites offered by numerous silver particles, which was responsible for the excellent electrocatalytic activity of the Ag electrode. Overall, the experimental results indicate that the use of an Ag/Cu electrode is a viable alternative treatment for MBAA dehalogenation. Further in-depth study is required before the application of these novel electrodes for the dehalogenation of other organic halides.

Reference

1. Y.H. Xu, Y.H. Zhu, F.M. Zhao and C.A. Ma, *Appl. Catal., A*, 324 (2007) 83
2. N.C. Ross, R.A. Spackman, M.L. Hitchman and P.C. White, *J. Appl. Electrochem.*, 27 (2007) 51
3. C.H. Lin and S.K. Tseng, *Chemosphere*, 39 (1999) 2375
4. S. Rondinini, P.R. Mussini, M. Sperchia and A. Vertova, *J. Electrochem. Soc.*, 148 (2001) 102
5. R. Chetty, P.A. Christensen, B.T. Golding and K. Scott, *Appl. Catal., A*, 271 (2004) 185
6. G. Chen, Z.Y. Wang and D.G. Xia, *Electrochem. Commun.*, 6 (2004) 268
7. R. Chetty, P.A. Christensen and B.T. Golding, *Chem. Commun.*, (2003) 984
8. H. Cheng, K. Scott and P.A. Christensen, *Environ. Sci. Technol.*, 38 (2004) 638
9. A.Matsunaga and A. Yasuhara, *Chemosphere*, 59 (2005) 1487
10. S. Rondinini, P.R. Mussini, P. Muttini and G. Sello, *Electrochim. Acta*, 46 (2001) 3245
11. Y.A. Zhuang, S. Ahn and R.G. Luthy, *Environ. Sci. Technol.*, 44 (2010) 8236
12. Y.S. Keum and Q.X. Li, *Environ. Sci. Technol.*, 39 (2005) 2280
13. J.Z. He, K.R. Robrock and L. Alvarez-Cohen, *Environ. Sci. Technol.*, 40 (2006) 4429
14. C.Y. Sun, D. Zhao, C.C. Chen, W.H. Ma and J.C. Zhao, *Environ. Sci. Technol.*, 43 (2009) 157
15. G. Soderstrom, U. Sellstrom, C.A. De Wit and M. Tysklind, *Environ. Sci. Technol.*, 38 (2004) 127
16. P. Dabo, A. Cyr, F. Laplante, J. Franklin, H. Ménard and J. Lessard, *Environ. Sci. Technol.*, 34 (2000) 1265
17. N.L. Stock and N.J. Bunce, *Can. J. Chem.*, 80 (2002) 200
18. G. Chen, Z.Y. Wang, T. Yang, D.D. Huang and D.G. Xia, *J. Phys. Chem. B*, 110 (2006) 4863
19. A.A. Isse, G. Berzi, L. Falciola, M. Rossi, P.R. Mussini and A. Gennaro, *J. Appl. Electrochem.*, 39 (2009) 2217
20. A.A. Isse, S. Gottardello, C. Durante and A. Gennaro, *Phys. Chem. Chem. Phys.*, 10 (2008) 2409
21. M. Fedurco, C.J. Sartoretti and J. Augustynski, *Langmuir*, 17 (2001) 2380.
22. C. Cougnon and J. Sirnonet, *Platinum Met. Rev.*, 46 (2002) 95
23. P. Poizot, L. Laffont-Dantras and J. Simonet, *J. Electroanal. Chem.*, 622 (2008) 204
24. B. Yang, G. Yu and D.M. Shuai, *Chemosphere*, 67 (2007) 1361
25. P. Poizot, L. Laffont-Dantras and J. Simonet, *J. Electroanal. Chem.*, 624 (2008) 52
26. S.M.A. Shibli and V.S. Dilimon, *Int. J. Hydrogen Energy*, 33 (2008) 1104
27. C.A. Ma, H. Ma, Y.H. Xu, Y.Q. Chu and F.M. Zhao, *Electrochem. Commun.*, 11 (2009) 2133
28. A.I.Tsyganok, I. Yamanaka and K. Otsuka, *J. Electrochem. Soc.*, 145 (1998) 3844
29. A.I.Tsyganok and K. Otsuka, *Appl. Catal., B*, 22 (1999) 15
30. Y.X. Fang and S.R. Al-Abed, *Appl. Catal., B*, 80 (2008) 327

31. C.Y. Cui, X. Quan, H.T. Yu and Y.H. Han, *Appl. Catal., B*, 80 (2008) 122
32. I.G. Casella and M. Contursi, *Electrochim. Acta*, 52 (2007) 7028
33. K. Miyoshi, Y. Kamegaya and M. Matsumura, *Chemosphere*, 56 (2004) 187
34. H. Cheng, K. Scott and P.A. Christensen, *J. Electrochem. Soc.*, 150 (2003) 17
35. B. Yang, G. Yu and X.T. Liu, *Electrochim. Acta*, 52 (2006) 1075
36. Z.R. Sun, B.H. Li, X. Hu, M.N. Shi, Q.Z. Hou and Y. Peng, *J. Environ. Sci.*, 20 (2008) 268
37. F. Alonso, I.P. Beletskaya and M. Yus, *Chem. Rev.*, 102 (2002) 4009
38. M. Fedurco, L. Coppex and J. Augustynski, *J. Phys. Chem. B*, 106 (2002) 2625
39. B. Yang, S. Wang, G. Yu and Y.R. Zhou, *Sep. Purif. Technol.*, 63 (2008) 353